

# Endmember Extraction for Pigment Identification Pre- and Post-intervention: A Case Study from a XVIth Century Copper Plate Painting

Ana B. López-Baldomero\*, Miguel A. Martínez-Domingo, Javier Hernández-Andrés, Rosario Blanc, J. L. Vilchez-Quero, Ana López-Montes, Eva M. Valero; University of Granada; Granada, Spain.\*:Department of Optics. Campus Fuentenueva, s/n 18071 Granada, Spain; anabelenlb@ugr.es

## Abstract

Three endmember extraction methods (NFINDR, NMF and manual extraction) are compared in two stages (pre- and post-intervention) of the same painting, a Maternity on copper plate, under study for the formulation of a hypothesis on the authorship and the dating. The endmembers are extracted from spectral images in the 400-1000 nm range. The main aim is to determine if simple automatic endmember extraction is enough for pigment and re-painted areas identification in this case study.

## Introduction

Pigment identification from spectral imaging data has been extensively explored in recent years [1-5]. From simple approaches like identifying features of the first and second-derivative spectra [3,6] to using optimal spectral bands selected for a particular set of pigments [7] or applying Deep Learning algorithms [8-11], many perspectives and solutions have been proposed. In most cases, a reference collection of prepared patches is needed, and often they must be prepared specifically for the substrate used in the painting to be analyzed. Despite all these contributions to the problem, it remains still challenging in many situations, and no universal consensus has been reached about a systematic way to approach it for real pieces of artwork. Some of the reasons that explain why a satisfactory solution has not yet been reached are the following:

1. The state of the piece. Pigment identification is mostly useful before a planned intervention, to identify the materials employed by the artist or else previous conservation activities. But the piece often is covered by a patina of unclean varnish which strongly darkens and alters the reflectance of the pigments, especially for mediaeval or renaissance paintings. Some studies have been done to predict the reflectance spectra of paintings after the removal of aged and discolored varnishes (i.e. virtual cleaning) [12,13]. The main problem with the proposed methods is the need for unvarnished areas in the paintings, or the removal of the varnish if these are not present, which is not always possible.

2. The presence of pigment mixtures. Pure pigments are seldom present in real artworks. In many situations, it is not practical to go on extending the number of reference pigments in the auxiliary patch collection until one covers all the possible mixtures that a given artist (often unknown) might have used. Then, spectral unmixing and endmember extraction techniques borrowed from the field of satellite imaging can be potentially helpful. They have been used in some previous studies [14,15] with variable degrees of success.

In this work, we aim to present a case study that is affected by these two problems, and demonstrate how unmixing techniques can be at least partially successful both for pigment

identification and gathering information about re-paintings present in the piece. The painting is on a somewhat unusual substrate (a copper plate) and shows a typical Maternity scene with the Virgin, an infant Jesus on her lap and St. Joseph on the right upper corner. This painting is under study for the formulation of a hypothesis on the authorship and dating by a multidisciplinary group (heritage restoration, art historians, mineralogy, optics, computer science and chemistry). This piece has further interest because it has recently been submitted to a restoration intervention that has removed the previous darkened patina of badly applied varnish, covered some missing areas (faults) by repainting, and applied a new varnish layer (see Figure 1 right). The visual appearance of the piece has noticeably changed after the intervention.



**Figure 1.** False RGB images of the Maternity painting object of this study. Left: before intervention. Right: after intervention. The size of the painting is 13,5x17,5 cm.

The piece presents a simple palette with five main pigments: Bones Black (BB), Lead White (LW), Cinnabar (CN), Naples Yellow (NY) and Lapislazuli (LL). They have been identified with X-Ray Fluorescence and X-Ray Diffraction analysis carried out by the Department of Analytical Chemistry of the University of Granada (the results are in the process of publication). The relatively short number of pigments used makes this piece a good case study for demonstrating the possibilities of unmixing techniques to tackle pigment identification pre-intervention. Also, the opportunity to study it after restoration will highlight the possibilities of these techniques and determine if spectral imaging in general is a good tool to identify areas that have been intervened.

We aim to produce some evidence about the best approaches for automatic endmember extraction and pigment identification from the list of endmembers using an auxiliary sample collection on the same substrate. In addition to this, we will compare the results between the original and restored

painting. Some novel features in the unmixing optimization procedure are also introduced.

## Methods

The provenance of the painting is a private collection in Spain. Two spectral images of the painting (pre- and post-intervention) were acquired in the visible and near infrared (VNIR range, from 400 to 1000 nm approx.) by a Resonon Pika L device, with a spatial resolution of 900 pixels per line and a spectral resolution of 2.1 nm. A sampling interval of 5 nm was used. The small size of the painting allowed the capture to be taken using a linear stage under halogen illumination. After spectral binning is used, the final size of the images [MxNxλ] is: [1111x881x121].

Once the spectral images were captured, three methods for endmember extraction were used: NFINDR [16], Non-negative Matrix Factorization (NMF) [17] and manual extraction of spectra in selected areas from the painting that appeared to contain each of the five pigments in its most pure form, although this was not possible for the Naples Yellow pigment, which appeared exclusively in mixed form.

An auxiliary copper plate was cleaned, sanded, and prepared using garlic and a mixture of linseed oil and Gesso, a procedure used during the XVI century. Another preparation layer was deposited with a mixture of Lead White, Black Bones and Red Earth. On this preparation, samples of each of the pigments (from Kremer Pigmente GmbH) were deposited, as well as several mixtures. The copper plate contained all the pigments present in the painting (LW, BB, LL, NY and CN) plus Azurite (AZ). Three mixtures were also prepared: REP+LW+BB (P1), LW+CN, and LW+LL. Spectral reflectances of deposited pigments and mixtures are shown in Figure 2. The information obtained by X-Ray Fluorescence and X-Ray Diffraction will serve as ground truth for the spectral analysis of the paintings.

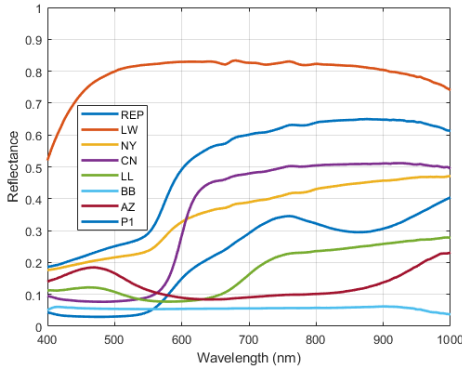


Figure 2. Spectral reflectance of the auxiliary copper plate.

Three sets of endmembers are extracted from the spectral images of the painting, and unmixing is carried out using non-linear optimization with a cost function based on a combined metric formed by two components: the complement of the Goodness-of-Fit coefficient (cGFC) and the Root Mean Square Error (RMSE). cGFC is sensitive to shape changes, while RMSE is sensitive both to scale and shape changes. The final form of the metric is:

$$M = cGFC + \alpha RMSE \quad (1)$$

Where  $\alpha = 1.0936$  (obtained using a preliminary round of optimization), which ensures that in average both metrics will contribute approximately equally to the final result.

The optimization algorithm is the interior point [18] with the sum-to-one constraint and a lower bound for the weights  $w_i$  of zero. The mixing model is a subtractive model [19]:

$$Y = \prod_{i=1}^q \rho_i^{\alpha_i} \quad (2)$$

Where  $Y$  is the spectral reflectance of the mixture,  $q$  is the number of candidate endmembers,  $\rho_i$  is the spectral reflectance of the  $i$ th endmember, and  $\alpha_i$  is its concentration. Both NMF and NFINDR have the limitations of a linear mixing model assumption, while subtractive mixing has been proven to be performing best for pigments on canvas [2]. On the other hand, the manual endmember extraction from the painting has the limitation of not corresponding to pure pigments and being affected by ageing. The unmixing process will estimate the weights in the mixture, and from them, we obtain the concentration maps and the error maps of the five endmembers (see Figure 4). This will allow us to identify which is the endmember set that works best for the spectral reconstruction of the painting using endmembers and estimated weights. This will be evaluated using both spectral and colorimetric differences on a pixel-by-pixel basis (cGFC, RMSE and CIEDE00) [20,21].

Finally, we will use the auxiliary set of reference spectra for trying to find the pigment that presents the closest spectral distance to each endmember for the three endmember extraction procedures. This spectral distance is calculated using a combined distance metric between the pigments in the plate and the endmembers obtained:

$$Mld = cGFC + 0.5MSE + 0.02\Delta E_{00} \quad (3)$$

The coefficients are obtained using the following tolerances for the three components of the metric: 0.01 for cGFC, 0.02 for MSE and 0.5 for  $\Delta E_{00}$ . Those coefficients ensure all the factors would contribute equally to the metric value in an acceptable reflectance match. After computing this metric, the label corresponding to the reference pigment with the minimum  $Mld$  metric value is assigned to each endmember. Finally, the hit rate is calculated as the percentage of correctly identified pigments with respect to the total number of pigments present.

The process will be repeated for the restored painting, allowing us to see if there are any differences in the performance of the unmixing algorithm, and if the renovated areas can be identified from the concentration maps.

All the calculations have been performed using MATLAB® (2022a version). The NFINDR and NMF algorithms used are those provided by MATLAB®, and the *fmincon* function is used for the unmixing optimization.

## Results

### Concentration maps and endmember sets

The endmembers (EM) sets differ for the three endmember extraction methods, and are not directly similar to the reference pigments (obtained with the auxiliary copper plate) in all cases, similarly to the findings in [7]. In Figure 3, the endmembers extracted from the painting pre- and post-intervention are shown. NMF algorithm implemented in MATLAB® provided EM reflectances with maximum values over 1, so they were normalized by the maximal value. The spectral reflectances are flatter for the manually extracted library than for those extracted with NFINDR or NMF algorithms. In general, post-intervention EM reflectances show lower values than pre-intervention

reflectances. This could be due to the removal of the whitish patina present in the original painting during the restoration process. NMF seems to provide reflectance curves that differ more from real pigments, so the preliminary hypothesis is that NFINDR and manual library will work best for the concentration vector and spectral estimation part of the unmixing process.

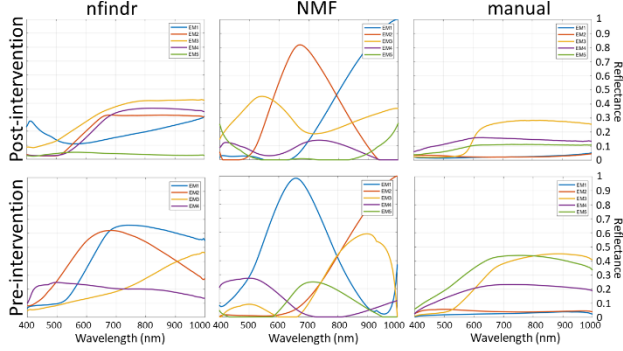


**Figure 3.** Endmember libraries extracted using NFINDR (left), NMF (center) and manual extraction (right) methods pre- (lower row) and post-intervention (upper row).

### Pre-intervention

Based on FRX and DRX results, CN can be detected in the Virgin's dress as well as the carnations, LL is present in both the background and the Virgin's mantle, LW is present in the carnations and the sleeves of the Virgin's chemise, NY can be detected in certain parts of the carnations and the Child's cloth, and BB is found in the background and shadowed areas. In Figure 4, concentration maps for the endmember (EM) most similar to Cinnabar (CN) in the three sets are shown for the unrestored painting (EM1 in NFINDR, EM2 in NMF, and EM3 in the manual extraction set). It can be seen that manual extraction method identifies the copper substrate as Cinnabar. NMF detects Cinnabar in the background, not only the dress and the carnations.

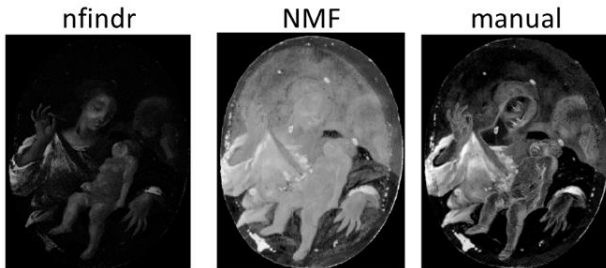


**Figure 4.** Concentration maps for the endmember most similar to Cinnabar in the pre-intervention painting. Left: NFINDR. Center: NMF. Right: manual extraction.

According to the concentration maps, EM3 obtained with NMF seems to represent the LL pigment, as well as EM4 in NFINDR (although this is less clear) and EM2 in the manual extraction. EM4 and EM5 in the manual extraction could represent the LW pigment, as well as EM2 in NFINDR, and EM1 in NMF (although it appears all over the painting).

### Post-intervention

In Figure 5, concentration maps for the endmember most similar to Cinnabar (CN) in the three sets are shown for the restored painting (EM4 in NFINDR, EM2 in NMF, and EM3 in the manual extraction set). Similar to the results obtained in the pre-intervention painting, the NMF method detects Cinnabar in

the background. The manual and NFINDR concentration maps seem plausible to the Cinnabar pigment, finding a higher concentration in the dress with the manual extraction method. In this state of the painting and according to the concentration maps, EM4 obtained with NMF seems to represent the LL pigment, as well as EM1 in NFINDR and EM2 in the manual method.

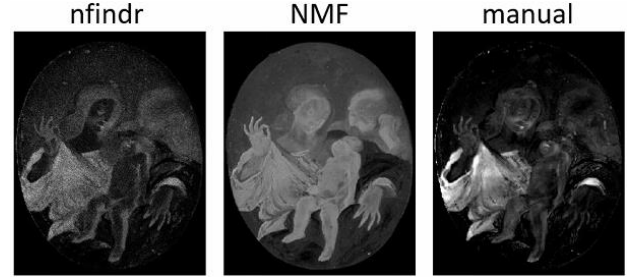


**Figure 5.** Concentration maps for the endmember most similar to Cinnabar in the post-intervention painting. Left: NFINDR. Center: NMF. Right: manual extraction.

### Spectral estimation quality

The RMSE error maps calculated from the differences between the reconstructed spectra using eq. (2) and the spectra from the spectral image of the unrestored painting are shown in Figure 6. Note that the range of values for RMSE is restricted to [0,1] for reflectance data. The mean RMSE value shows that NFINDR fails to provide an accurate spectral reconstruction, while the manual extraction produces the best results.

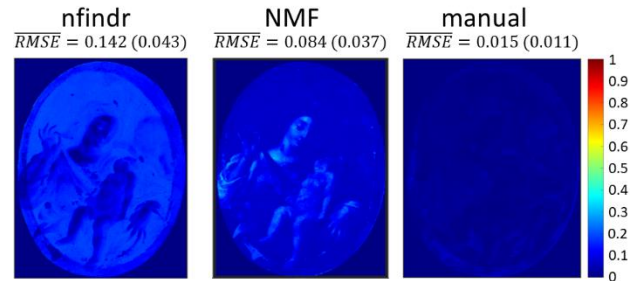


**Figure 6.** RMSE error maps for the pre-intervention painting. Mean (and standard deviation) values are shown on top of each map. Left: NFINDR. Center: NMF. Right: manual extraction.

The cGFC error maps for the restored painting are shown in Figure 7. We can see that NMF method fails to reconstruct the shape of the spectra compared to manual extraction and NFINDR.

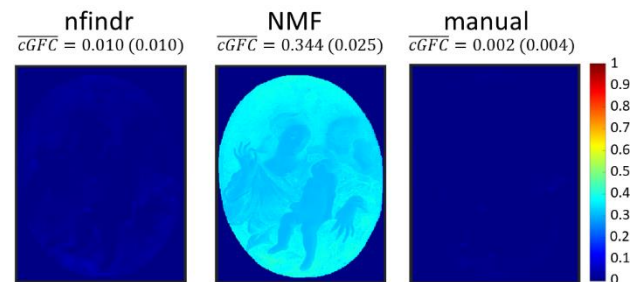


**Figure 7.** cGFC error maps for the post-intervention painting. Mean (and standard deviation) values are shown on top of each map. Left: NFINDR. Center: NMF. Right: manual extraction.

In Table 1, the cGFC, RMSE and  $\Delta E_{00}$  values obtained from the comparison between the estimated and the original spectra are shown for each endmember (EM) set and state of the



painting. The best cGFC, RMSE and  $\Delta E_{00}$  values are obtained in both states for the manual extracted library. Comparing the painting pre- and post-intervention, lower values for cGFC are found for the pre-intervention painting with the NMF and NFINDR libraries. Comparing the RMSE values, post-intervention painting provides the lowest values for all three quality metrics. For the  $\Delta E_{00}$ , the values depend on the endmember extraction method used, not so much influenced by the painting state. For the post-intervention painting, the mean cGFC value and the error map (Figure 5 lower row) show that NMF is the worst algorithm in providing accurate spectral reconstruction. Comparing the results with manual and NFINDR extraction methods, the manual method is 5 times better than NFINDR in terms of cGFC. Our preliminary hypothesis, i.e., that NFINDR and manual libraries will work better than the NMF library, is true for the cGFC and the  $\Delta E_{00}$ , but not for the RMSE. This means that the NMF algorithm introduce some additional changes in shape in the estimated spectra with respect to the original, but overall, it is better than NFINDR at capturing the scale of the spectral reflectances. This could be because NFINDR is more sensitive to the problem of using a linear mixture model for EM extraction than NMF.

**Table 1. Spectral estimation quality metrics for the three endmember sets pre- and post-intervention**

	EM set	cGFC (STD)	RMSE (STD)	DE00 (STD)
Pre-intervention	NFINDR	0.007 (0.005)	0.142 (0.043)	19.72 (6.28)
	NMF	0.296 (0.030)	0.084 (0.037)	23.87 (5.34)
	Manual	0.005 (0.008)	0.015 (0.011)	3.94 (2.52)
Post-intervention	NFINDR	0.010 (0.010)	0.074 (0.031)	12.64 (5.12)
	NMF	0.344 (0.025)	0.073 (0.023)	29.38 (3.28)
	Manual	0.002 (0.004)	0.014 (0.0015)	4.17 (2.29)

### Pigment identification

Pigment identification results are shown using the reflectance of the pigments in the auxiliary copper plate as reference (Table 2).

**Table 2. Pigment identification results for the three endmember sets pre- and post-intervention**

	EM set	Assigned labels	Hit rate	Mld range
Pre-intervention	NFINDR	P1, REP, NY	20	0.29-0.53
	NMF	P1, REP, LL, AZ	20	0.61-0.79
	Manual	BB, REP, NY	40	0.14-0.40
Post-intervention	NFINDR	LL, REP, NY, REP, BB	60	0.13-0.27
	NMF	LL, P1, LW, BB, AZ	60	0.506-0.875
	Manual	BB	20	0.11-0.42

Depending on the state of the painting, different results have been obtained with the three libraries. For the pre-intervention

painting, the best result is obtained with the manual library with a hit rate of 40%, compared to the 20% obtained with NFINDR and NMF libraries. Even being the best, it fails to identify CN, LW and LL. Referring to the post-intervention painting, the best results are obtained with NFINDR and NMF libraries, with a hit rate of 60%. Both identify LL and BB, NY is identified in NFINDR, and LW is identified in NMF. AZ is identified in NMF, but it is not present in the painting. In both states of the painting, NMF library shows the higher Mld values. Compared to the other libraries, the manual extracted library is inherently disadvantaged because the reflectances of the paintings are consistently much lower than those of the reference library. As a result, more than one EM is classified as BB, which does not happen with the other libraries. These results are conditioned by the restricted and specific set of pigments used in the copper plate, which contains seven pigments and three mixtures.

### Identification of re-painted areas

First, renovated areas were searched from the concentration maps of the restored painting. They seemed to appear in the EM1 of the NMF library (Figure 8 left) in the form of small white spots, and in the EM2 of the same library and the EM3 of the manual extracted library as black spots. The restored areas were not easily visible in the other concentration maps and libraries.

Due to the slightly different color showed by the re-painted areas, we decided to search the best three bands of the spectral cube that provided the higher F-score value (see eq. (4)) comparing the false RGB image to a ground-truth (GT) of re-painted areas obtained manually from the original painting. The segmentation of re-painted areas was performed in the false RGB color space, looking for the optimum minimum and maximum values for the three channels. In a preliminary study, we performed a band-by-band intensity thresholding, but the results were worse than those obtained with a color-based segmentation. The optimization was done with the functions *surrogateopt* and *genetic algorithm (GA)*, implemented in MATLAB®.

$$F\text{-score} = 2 \frac{\text{precision} \cdot \text{recall}}{\text{precision} + \text{recall}} \quad (4)$$



**Figure 8.** Concentration map for the EM 1 obtained with NMF (left). False RGB image of the restored painting with channels [695,980,905] nm (right).

For the *surrogateopt*, the best combination of three bands was [410,965,705] nm. The minimum and maximum RGB values were: [(75,94), (17,162), (23,129)] for red, green, and blue respectively, and the best F1 score value was 0.112. For the *GA*, the best combination of three bands was [695,980,905] nm (Figure 8 right). Re-painted areas can be seen with a light green

color against the background. The minimum and maximum thresholds in RGB were: [(36,91), (133,175), (106,194)], and the best F1 score value was 0.170. The best results were obtained with *GA*, although they were not good for any of the optimizations. This makes sense because *GA* is a global optimizer while *surrogateopt* attempts to find the global minimum using few objective function evaluations, which can lead to a local instead of a global solution. The main advantage of *surrogateopt* is the reduced computational cost and executing time.

To improve the results obtained in the detection of re-painted areas in a restored painting with VISNIR information, it could be beneficial to use the SWIR (short-wavelength infrared) range, since this type of radiation can penetrate more deeply into the different layers of the painting.

## Discussion and conclusions

In this study, three endmember extraction methods (NFINDR, NMF and manual extraction) are compared in two stages (pre- and post- intervention) of the same painting. The spectral images of the painting were captured from 400 to 1000 nm. Pigment identification was also conducted using an auxiliary set of reference spectra on the same substrate and with the same preparation, but corresponding to new materials.

The endmembers obtained from the manual extraction method were flatter than those obtained with NFINDR and NMF methods. The reflectance curves of the NMF endmembers differed from real pigments. The best concentration maps (i.e. those most similar to the real pigment distributions) were obtained with the manual extraction method.

Attending to the spectral reconstruction of the three endmember extraction methods, manual extraction performed the best, with the lowest values of cGFC, RMSE and  $\Delta E_{00}$  for both states of the painting. Comparing the painting pre- and post-intervention, lower values for cGFC were found for the pre-intervention painting with the NMF and NFINDR libraries, but RMSE was lower in the post-intervention case. This can maybe be linked to the fact that the renovated painting is more inhomogeneous than the original painting, and the spectral reconstruction is harder for this sample. The RMSE values can be explained because the highest reflectance values correspond to NMF, and this is an initial advantage to get the scale right in the spectral reconstruction. NFINDR and manual libraries worked better than the NMF library considering the cGFC and the  $\Delta E_{00}$ , but not for the RMSE.

The results of pigment identification were influenced by the state of the piece. Manual extraction performed the best for the unrestored painting, identifying only two pigments, while NFINDR and NMF performed the best for the restored painting, identifying three over five pigments. The manually extracted endmembers differ more from the reference library for the pre-intervention painting than for the restored one. This explains the overall worse identification results for the first case. However, restoring the piece enhances the efficiency of automatic algorithms in extracting endmembers for pigment identification (not for reconstruction of the spectra, which is inherently more difficult). This highlights the disadvantage of the manual extracted library compared to the automatically extracted ones. Even with a very reduced palette of pigments, the results were not as expected. This could be due to differences between the spectra of the reference pigments and the actual pigments present in the painting. These findings underscore the importance of having an appropriate auxiliary palette of reference pigments for pigment identification.

The comparison of the information present in the concentration maps obtained from the unmixing process does not

appear to be sufficient for detection of re-painted areas. Even after finding the triplet of spectral bands that produced a more salient visualization of the repainted areas with an optimization approach, the results obtained by thresholding were not similar enough to the ground truth image containing all the repainted areas.

The limitations imposed by linear unmixing could be addressed by using a Kubelka-Munk model to approximate the reflectance of mixed pigments. More sophisticated segmentation algorithms to detect re-painted areas could also be considered in future work, as well as information in different spectral ranges.

Spectral image capture is totally non-invasive, has high spatial resolution and requires much less time for capture and analysis than alternative techniques, which underscore the importance of devoting more effort to refining spectral imaging and unmixing methods so that they can perform well in endmembers extraction and pigment identification.

## References

- [1] F. Grillini, J.B. Thomas and S. George, "VisNIR pigment mapping and re-rendering of an experimental painting," *JAIC*, 26, 3-10 (2021).
- [2] F. Grillini, J.B. Thomas and S. George, "Comparison of Imaging Models for Spectral Unmixing in Oil Painting," *Sensors*, 21(7), 2471 (2021).
- [3] R. Radpour, G.A. Gates, I. Kakoulli and J.K. Delaney, "Identification and mapping of ancient pigments in a Roman Egyptian funerary portrait by application of reflectance and luminescence imaging spectroscopy," *Herit. Sci.*, 10(1), 1-16 (2022).
- [4] J.K. Delaney, K.A. Dooley, A. Van Loon and A. Vandivere, "Mapping the pigment distribution of Vermeer's Girl with a Pearl Earring," *Herit. Sci.*, 8(4), 1-16 (2020).
- [5] A. Bentkowska-Kafel and L. MacDonald, *Digital Techniques for Documenting and Preserving Cultural Heritage* (Arc Humanities Press, Leeds, 2018) pg. 141-158.
- [6] L. Jin-xing and W. Xiao-xia, "Non-destructive pigment identification method of ancient murals based on visible spectrum," *Spectrosc. Spect. Anal.*, 37(8), 2519-2526 (2017).
- [7] J. Cai, H. Chatoux, C. Boust and A. Mansouri, "Extending the Unmixing methods to Multispectral Images," *Proc. CIC*, pg. 311-316. (2021).
- [8] N. Rohani, E. Pouyet, M. Walton, O. Cossairt and A.K. Katsaggelos, "Pigment unmixing of hyperspectral images of paintings using deep neural networks," *Proc. ICASSP*, pg. 3217-3221. (2019).
- [9] B. Rasti, B. Koirala, P. Scheunders and J. Chanussot, "Minsicnet: Minimum simplex convolutional network for deep hyperspectral unmixing," *IEEE Trans. Geosci.*, 60, 1-15 (2022).
- [10] L. Qi, J. Li, Y. Wang, M. Lei and X. Gao, "Deep spectral convolution network for hyperspectral image unmixing with spectral library," *Signal Process.*, 176, 107672 (2020).
- [11] T. Kleynhans, C.M. Schmidt Patterson, K.A. Dooley, D.W. Messinger and J.K. Delaney, "An alternative approach to mapping pigments in paintings with hyperspectral reflectance image cubes using artificial intelligence," *Herit. Sci.*, 8(1), 1-16 (2020).
- [12] G. Trumpy, D. Conover, L. Simonot, M. Thoury, M. Picollo and J.K. Delaney, "Experimental study on merits of virtual cleaning of paintings with aged varnish," *Opt. Express*, 23(26), 33836-33848 (2015).
- [13] C.M.T. Palomero and M.N. Soriano, "Digital cleaning and "dirt" layer visualization of an oil painting," *Opt. Express*, 19(21), 21011-21017 (2011).
- [14] H. Deborah, M.O. Ulfarsson and J. Sigurdsson, "Fully Constrained Least Squares Linear Spectral Unmixing of The Scream (Verso, 1893)," *Proc. 11<sup>th</sup> WHISPERS*, pg. 1-5. (2021).
- [15] J. Cai, H. Chatoux, C. Boust and A. Mansouri, "Comparison of Linear Unmixing Methods on Paintings Data Set," *Proc. ORASIS* 2021, pg. 1-9. (2021).
- [16] M.E. Winter, "N-FINDR: An Algorithm for Fast Autonomous Spectral End-Member Determination in Hyperspectral Data," *Proc. Imaging Spectrometry V*, pg. 266-275. (1999).
- [17] Y. Li and A. Ngom, "The non-negative matrix factorization toolbox for biological data mining," *Source Code Biol. Med.*, 8(1), 1-15 (2013).
- [18] R.A. Waltz, J.L. Morales, J. Nocedal and D. Orban, "An interior algorithm for nonlinear optimization that combines line search and trust region steps," *Math. Program.*, 107(3), 391-408 (2006).
- [19] S.A. Burns, "Subtractive color mixture computation," *arXiv preprint arXiv:1710.06364*, (2017).
- [20] J. Hernández-Andrés and J. Romero, "Colorimetric and spectroradiometric characteristics of narrow-field-of-view clear skylight in Granada," *JOSA A*, 18(2), 412-420 (2001).
- [21] F.H. Imai, M.R. Rosen and R.S. Berns, "Comparative study of metrics for spectral match quality," *Proc. CGIV*, pg. 492-496. (2002).

## Author Biography

**Ana B. López-Baldero** is a Ph.D. candidate at the Color Imaging Lab (University of Granada). She obtained her B.Sc. in Optics and Optometry in 2019 at the University of Granada, where she also obtained both her M.Sc. in Clinical Optometry and Advanced Optics in 2020, and her M.Sc. in Physics in 2021. Her current research focuses on hyperspectral image acquisition and analysis for the identification of materials in historical documents.

**Miguel Ángel Martínez-Domingo**, obtained his PhD. in Physics and Space Science in 2017. He is graduated in Telecommunications Engineering and Optics. He is currently Assistant professor at the Department of Optics of University of Granada and member of the Color Imaging Lab. His research interests are focused on spectral imaging applied to cultural heritage, color vision and food inspection among others.

**Javier Hernández-Andrés**, who obtained a Ph.D. in Physics in 1999, is Full Professor at the University of Granada since 2016 and a member of the Color Imaging Lab. His recent research focuses on color vision, color imaging and hyperspectral imaging. Currently he is associate editor for "Optics Express" and member of the editorial board of "Color Research and Application".

**M. Rosario Blanc** has worked at the Department of Analytical Chemistry at the University of Granada as Assistant Prof. from 1986 to 2003, as Associate Prof. from 2003 to 2021 and as Professor from 2021. She's a member of the Analytical Chemistry and Life Sciences research group. Her research work has been focused on the development of new analytical methodologies for the study and determination of materials and the study of the degradation processes of artworks.

**J.L. Vilchez-Quero** Ph.D. in Analytical Chemistry. Postdoctoral scholarship at the University of Madrid. Research Fellow at the Oklahoma State University (1988). Full Professor of Grenade University from 1998. Supervisor of radioactive facilities from 2015. He founded the research group "Analytical Chemistry and Life Sciences" (1995). His research interest was environment, drugs and recently the analysis of materials of works of art (Pigments, Colorants and Binders). He is Editor of several scientific journals.

**Ana López-Montes** received her B. Sc. in Fine Arts with the specialization on Restoration at the University of Granada (Spain) in 2001. In 2006 she was awarded her Doctorate in Fine Arts and in 2015 a second Doctorate in Analytical Chemistry. She carried out her post-doctoral stays in IRAMAT-CNRS (Orléans, France) and in CRC-CNRS (Paris, France). She has worked at the Department of Painting at the University of Granada as Associate Professor from 2019.

**Eva M. Valero** obtained a B.D. in Physics in 1995, and a Ph.D. in 2000, both at the University of Granada. She has worked at the Department of Optics as Assistant Prof. from 2001 to 2007 and as Associate Prof. from 2007. She's a member of the Color Imaging Lab at the University of Granada. Her research interests were initially spatial color vision, and more recently multispectral imaging and color image processing.